Experimental Study of Oil-Water Flow Patterns in a Large Diameter Flow Loop—The Effect on Water Wetting and Corrosion

Kok Eng Kee, Sonja Richter,* Marijan Babic,* and Srdjan Nešić‡,**

ABSTRACT

Carbon steel pipelines are commonly used in transporting hydrocarbon products. In offshore oilfields, the produced crude oil generally contains water flowing concurrently in the flowlines. The presence of water can lead to internal corrosion problems when free water is in contact with the pipe wall surface. Hence, it is pertinent to study how the distribution of water under different oil-water flow conditions could affect the surface wetting on the steel pipe, i.e., whether the wall surface is wetted by water or oil phase. In this experimental work, a large scale 0.1 m (4 in) internal diameter inclinable flow loop was used to study the two phase oil-water flow in horizontal and vertical positions. Paraffinic light model oil (40°API) and 1 wt% NaCl aqueous solutions were utilized as the test fluids. Two measurement techniques, flush mounted conductivity pins and high-speed camera, were used for surface wetting determination and flow patterns visualization, respectively. The wetting data were classified based on four types of wetting behaviors: stable water wet, unstable water wet, unstable oil wet, and stable oil wet. The wetting results from the conductivity pins were found to match with the visualization results from the high-speed camera. The horizontal oil-water flow results showed that water flows separately and wets the pipe bottom at low mixture liquid velocity. In addition, not all of the water was fully entrained in high flow rate, as traces of water could still be found to wet the surface intermittently, causing unstable oil wetting. Based on the iron counts measurement, the corrosion rate was highest when the oil-water flow was laden with high water cut coupled with high flow velocity, corresponding to water wetting behavior.

KEY WORDS: conductivity pin, flow pattern, iron count, oil-water flow, water wetting, wettability

INTRODUCTION

In the oil industry, formation water is often produced along with the crude oil and transported in carbon steel pipelines. Some of the primary parameters in internal corrosion assessment of pipelines are the presence of free water and the content of corrosive species such as CO_2, H_2S, organic acids, etc. Because the corrosive species are soluble in the aqueous phase, the likelihood of internal corrosion increases when the water systematically separates out of the oil stream and comes into contact with the pipe wall surface, a scenario known as "water wetting." On the other hand, "oil wetting" takes place when the wall surface is wetted by oil phase and the water is entrained. Oil wetting retards the corrosion rate as the corrosive species do not come into direct contact the pipe wall. In an oil-water flow with oil as the dominant phase and water as the dispersed phase, varying degree of dispersion driven by the flow can lead to different flow regimes in the pipe. The water wetting of the internal pipe wall is closely related to how the water is distributed in the oil-water flow, and this affects the occurrence of internal corrosion.

The horizontal oil-water flow patterns can be classified into two broad categories: separated and dispersed flows, according to the distribution of the

Submitted for publication: April 27, 2015. Revised and accepted: December 21, 2015. Preprint available online: December 21, 2015, http://dx.doi.org/10.5006/1753.
‡ Corresponding author. E-mail: nesic@ohio.edu.
* Institute for Corrosion and Multiphase Technology, Ohio University, Athens, OH 45701.

ISSN 0010-9312 (print), 1938-159X (online)

phases.[1] At a low flow rate, the oil and water flow separately as continuous phases. Some degree of fluid mixing and entrainment may be present at the oil/water interface. Separated flow is typically observed in horizontal or near horizontal flow. As the oil flow rate increases, the flow has sufficient turbulence to break up the water phase into globules or droplets of varying size. Five oil-dominated flow patterns for water cut ranging up to 20% were observed. The spatial distribution of the phases are described below and illustrated in Figure 1.

Separated flow:

- *Stratified smooth (ST-S)* is a flow with continuous oil and water phases separated with a smooth interface. Entrainment of water is not observed.
- *Stratified with globules (ST-G)* occurs at a low water cut where swarms of closely packed water globules/droplets are seen moving at the lower half of the pipe. The mobility of the droplets is somewhat restricted as they agglomerate to move as a single unit.
- *Stratified with mixing layer (ST-M)* has a mixing layer flowing in the intermediate between the continuous oil and water phases. Both oil-in-water and water-in-oil dispersions exist in the mixing layer.

Dispersed flow:

- *Semi-dispersed (S/D)* is a form of dispersion where droplets are entrained as an inhomogeneous water-in-oil dispersion with an increased concentration toward the lower half of the pipe resulting from gravity.
- *Full dispersed (D)* occurs when water droplets are homogenously distributed across the pipe. The droplets are smaller and they appear to move as fast as the bulk oil flow.

By comparing the flow patterns with those nomenclatures proposed in Trallero's work, *stratified smooth* is equivalent to ST, *stratified with mixing layer* is ST & MI, *semi-dispersed* is Dw/o & o, *full dispersed* is w/o, while *stratified with globule* is not accounted for.[2] It is noted that perfectly horizontal pipelines seldom exist in the field. Any change in the pipe inclination may affect the phase distribution. For example, in an upward inclined pipe, water phase flows slower because of the gravity force pulling the denser phase down an inclined plane, resulting in an increased water holdup.

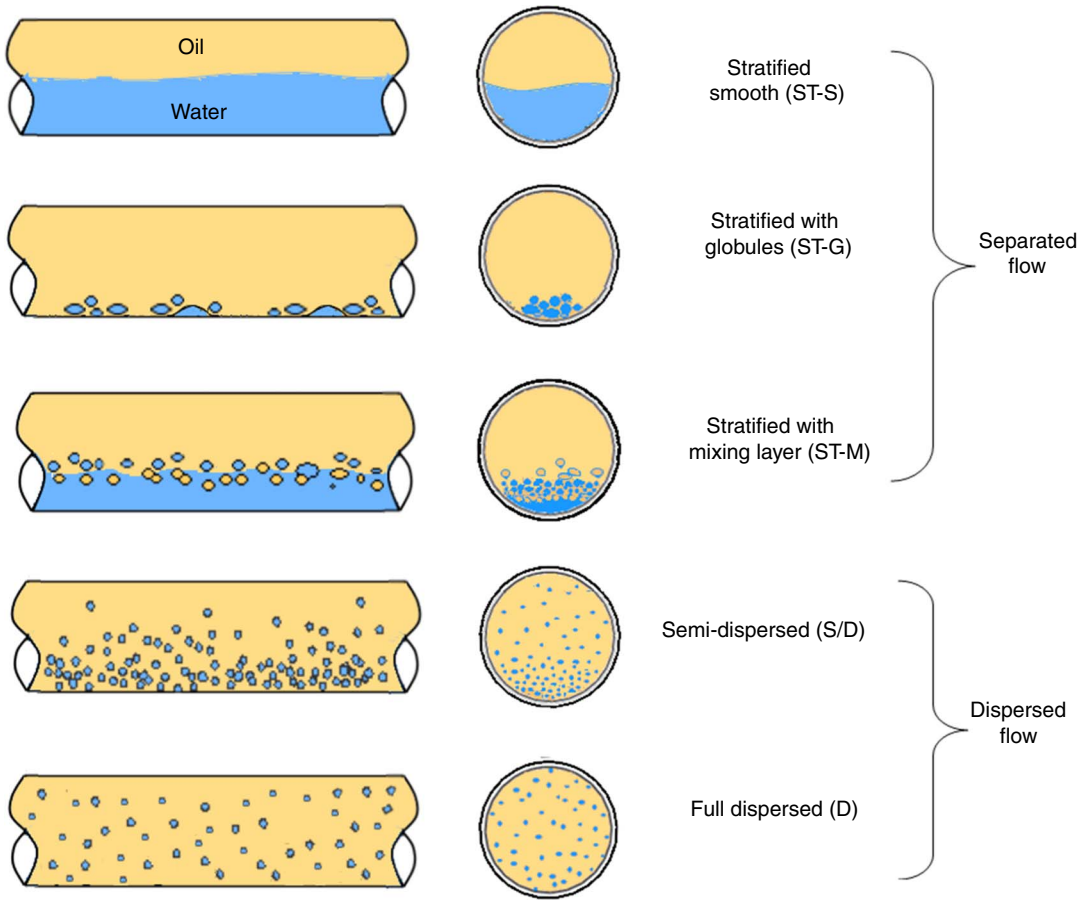

FIGURE 1. *Schematics of separated and dispersed flow patterns in horizontal oil-water flow.*

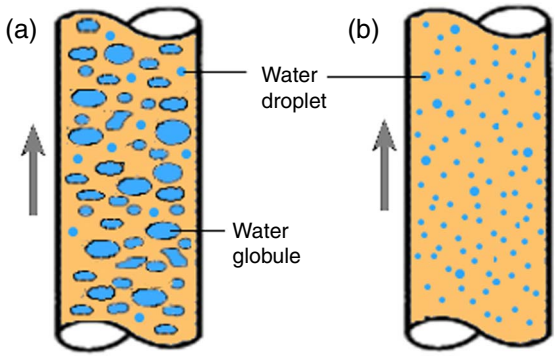

FIGURE 2. *Schematics of flow patterns in vertical oil-water flow: (a) dispersed globules flow pattern, and (b) dispersed droplets flow pattern.*

While separated flow can be observed in horizontal or near-horizontal pipe, it does not exist in vertical flow. Flores reported that the separated flow in a 2 in (0.05 m) internal diameter (ID) pipe did not exist if inclined more than 33°.[3] For the oil-dominated upward flow in vertical pipe, two subgroups of dispersed flow patterns, *dispersed droplets* and *dispersed globules*, as described in Flores' work, were observed here.[3] They are shown schematically in Figure 2.

- *Dispersed globules* are seen at low liquid velocity where large clusters of irregularly shaped blobs of water globules are intermixed with small spherical water droplets in the continuous oil flow. The droplets are fairly small and rounded, as governed by the surface tension. The larger globules are either in a flat oval or irregularly deformed shape. The large globules flow with significant slippage with respect to the bulk oil flow.
- *Dispersed droplets* occur at higher flow rate where small round water droplets are dispersed uniformly across the pipe. The droplets are seen to flow in a relatively straight path, almost as fast as the oil phase.

In horizontal oil-water flow, the pipe position at 6 o'clock (bottom of the pipe) is the most susceptible location to corrosion, as the water can drop out from the bulk oil phase and wet the pipe wall. In vertical oil-water flow, there is no preferential wetting location around the pipe circumference. There has been a number of large scale flow loop works done on the oil-water flow patterns and the hydrodynamic parameters such as pressure drop and liquid holdup.[2-6] Nonetheless, little or no emphasis was placed on the water wetting or distribution of the water phase in these studies. Electrically-based probes have been commonly used to identify the phase in multiphase flow environment.[7] Trallero used an array of conductance probes to identify the local phase continuity in a horizontal oil-water flow system.[8] Flores, et al., used five dual-electrode conductance probes that were installed at different radial distances to characterize the vertical and inclined oil-water flow patterns.[3] Valle used conductance probes to study the relation of water exposure and corrosion in oil-water flow system.[9] Angeli and Hewitt used a high-frequency impedance probe to detect the local phase continuity and a conductivity needle probe to determine the continuous phase in oil-water system.[10] Researchers at Ohio University engineered a large array of non-intrusive conductivity probes flush mounted onto the inner pipe wall to detect the water wetting behavior in oil-water flow system.[1,11-15]

EXPERIMENTAL DETAILS

The current work focused on the flow patterns, and water wetting behaviors were tested in a large-scale flow loop. Light paraffinic model oil (40°API) was used as the continuous phase and water as the secondary phase with water cut up to 20%. The experiments were conducted in an inclinable multiphase flow loop that can be used to study gas-liquid, liquid-liquid, or gas-liquid-liquid flow systems, as shown schematically in Figure 3. The main line of the flow loop was a 45 m long line, 0.1 m (4 in) ID pipe line mounted on a steel rig structure. It consisted of two parallel legs of polyvinyl chloride (PVC) pipe connected by a 180° bend. This section of the loop could be inclined from an angle of 0° (horizontal) to 90° (vertical). Oil and water fluids were pumped separately from the storage tanks into the main flow line by respective progressive cavity pumps. The oil flow was fed directly to the main line, while the water flow was directed to the main line via a tee section. The fluid mixture first flowed through a 3.6 m long flexible polyethylene hose, which allows for mixing and rig inclination before entering the first upstream leg of the main line. The mixture flowed for 100 pipe diameters to ensure fully developed flow before reaching the 1.8-m-long mild steel test section, used for surface wetting measurement, followed by a transparent PVC pipe section, used for flow pattern visualization. A photo of the upstream test sections is shown in Figure 4. Upon exiting the main line, the fluid mixtures were directed to a horizontal liquid-liquid separator for separation. The separated phase returned to the respective storage tank before being recirculated back to the flow loop. The oil phase used was a light refined paraffinic oil (commercial trade name: LVT200[†]), and the water phase used was 1 wt% NaCl solution prepared from deionized water and analytical grade reagent. The properties of the fluids are shown in Table 1.

High-Speed Camera

The flow pattern visualization was achieved by a high-speed video camera (model Vision Research Phantom V12.1[†]) that can capture the fast-motion multiphase fluid flow through the transparent PVC

[†] Trade name.

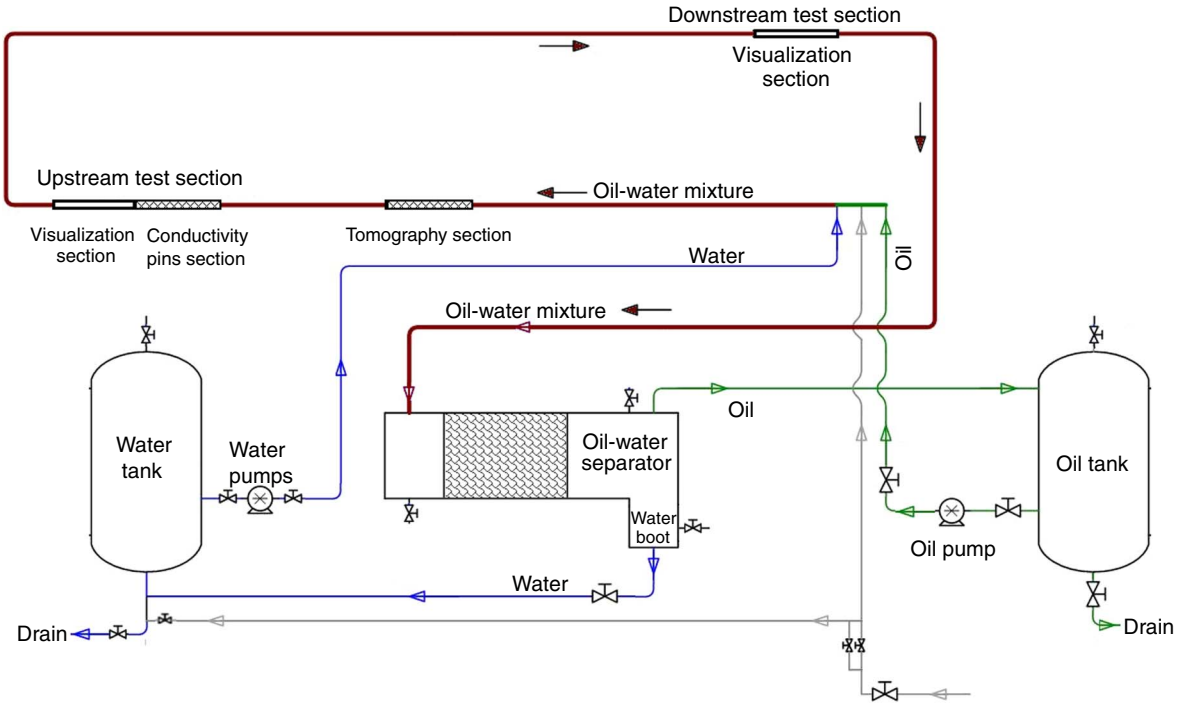

FIGURE 3. *Schematic layout of the inclinable 0.1 m ID flow loop used for oil-water flow.*

pipe. The camera has a 1,280×800 pixel complementary metal-oxide semiconductor (CMOS) sensor and was set up to record the flow at a framing rate of 6,000 frames/s (fps). During the experiment, one side of the pipe was illuminated with a high intensity light source, such that the illumination through the pipe would be positioned directly opposite the camera lens on the other side of pipe. A white sheet of translucent paper was placed in between to evenly diffuse the light. The settings adjustment and filming of the video files (in .cine format) were controlled through the cine video software in a host computer.

Conductivity Pins

The surface wetting was determined by use of conductivity pins, which were flush mounted onto the interior wall of 0.1 m ID carbon steel test section. Two types of pins sections were used with identical pin design and working principle. The difference is one section comprised 93 pins covering one-half (180°) of the pipe circumference (Figure 5[a]), named the 180° pins section, while the other comprised 160 pins covering the entire pipe circumference, named the 360° pins section. The 180° pins section was suited for horizontal flow, while the 360° pins section was for vertical flow. The array of pins flush mounted on the interior wall acted as the electrically-based sensors that discretely measured the electrical conductivity of the phase that wets the pin tip. The current pin design was an upgraded version of a previous pin design, used in previous work.[1] The original design was made of 20 AWG (American Wire Gauge) 0.032 in (0.81 mm) outer diameter (OD) stainless steel (SS) pin insulated with epoxy flushed mounted in a 1.6 mm (0.0625 in) hole. The original design suffered from galvanic corrosion because the electrical path was formed between the SS pin and the surrounding steel pipe wall, which were of dissimilar materials. The upgraded design comprised

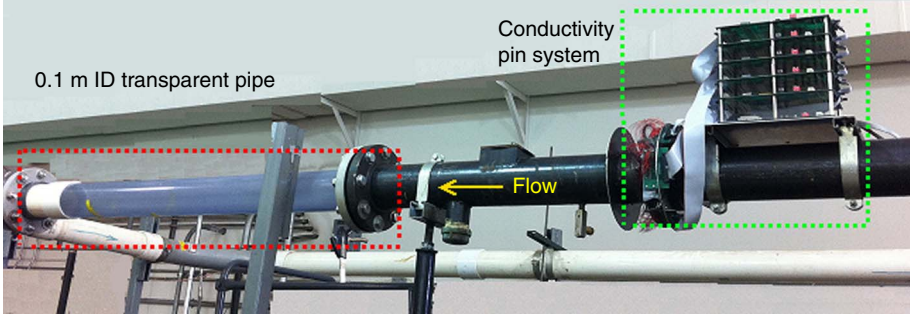

FIGURE 4. *The 0.1 m ID transparent pipe and pin test section fitted with conductivity pins.*

TABLE 1
Fluids Properties Used in This Work

Parameter	Value at 25°C	
	Oil Phase	Water Phase
Liquid phase	light refined paraffinic oil	1 wt% NaCl (aq.)
Density (kg/m^3)	823	1,000
Dynamic viscosity (cP)	2.7	1
Surface tension (mN/m)	28.5	72
Oil-water interfacial tension (mN/m)	40.5	
Water-in-oil contact angle (°)	73	

the same 20 AWG SS pin but was encased with epoxy in a 1.5 mm (0.06 in) SS sleeve. The assembly was then insulated with epoxy resin and flush mounted in a 1.6 mm (0.0625 in) hole.

During operation, all pins were excited with a square wave source voltage oscillating from 0 V to 4.5 V at 100 Hz. At this relatively low frequency, only the resistive element is measured in the circuit. When an exposed pin tip is bridged by conductive water, a low resistive circuit loop is formed between the inner pin electrode and the outer grounded pin sleeve. This results in a low voltage drop in that particular pin circuit, vice versa for a pin tip covered by the oil phase, which will result in higher voltage drop. The voltage response, V_{in}, can then be compared with a preset reference voltage V_{ref} in a voltage comparator circuit to produce a two-level signal. The V_{ref} value was calibrated against the salinity of the water used in the flow loop. Slightly saline water was favored to improve the signal quality. For each pin, the two-level signal logic for the surface wetting condition was interpreted as follows:

If $V_{in} \leq V_{ref} \Rightarrow$ water wet
If $V_{in} > V_{ref} \Rightarrow$ oil wet

These signals were processed by a data acquisition system in a microprocessor circuit. The local instantaneous signals of all pins were displayed by a conductivity pin program in a host computer as a pictorial wetting snapshot with time stamp, as shown in Figure 5(b). Before the start of the experiments, the test section was thoroughly polished to remove grimes/impurities deposited on the pins followed by continuous "rinsing" with gas-oil slug flow to condition the pins. A detailed description of the conductivity pin system and the test facility can be found elsewhere.[16]

One way to study the implication of surface wetting on corrosion of mild steel in an aqueous CO_2 environment is by measuring the change of soluble iron concentration in the water phase, often referred to as the "iron counts."[1,12] The soluble iron in water typically originates from corrosion—in the present case from oxidation of iron in the test section, which was the only component of the loop system made of mild steel, while the rest was made of non-corroding plastics. Prior to the experimentation, the internal wall of the mild steel test section was always polished with a cylinder hone to remove any residual corrosion scale. As the pin section is located approximately at mid distance of the 1.8-m-long test section, a silicon carbide cylinder hone (120 grit) with an extended stem driven by portable drill was used to polish the pin surface lubricated with water. The polishing duration was kept brief, to 3 min, and the polished pin section was then wiped clean with isopropanol to ensure the consistency of the pin surface. No attempts were made to measure the pipe surface finish. The liquids in the flow loop were continuously purged with CO_2 gas for 8 h to deoxygenate the system. The purged water pH typically stabilized at pH 4.4, while the dissolved O_2 concentration was around 0.5 ppm, as measured by the colorimetric test kit. Four flow conditions resulting in water wet, unstable water wet, and unstable oil wet

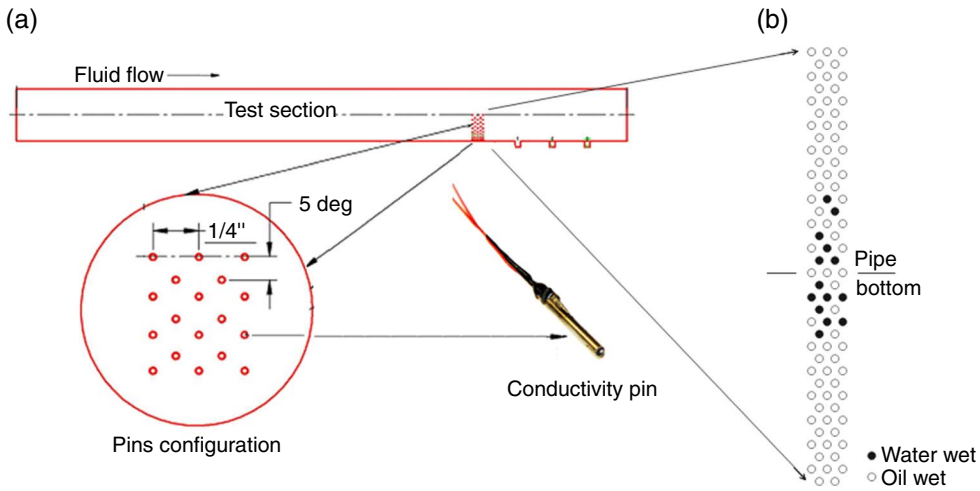

FIGURE 5. *(a) Schematic layout showing conductivity pin array flushed mounted on the internal wall of 180° pins section covering the lower half of the pipe circumference. (b) Typical wetting pins snapshot.*

TABLE 2
Test Matrix for Horizontal and Vertical Oil-Water Flow Experiments

Parameter	Value	
System conditions	1 atm (101.325 kPa) at 22°C	
Oil phase	light refined paraffinic oil	
Water phase	1 wt% aqueous NaCl	
Pipe ID (m)	0.1	
Inclination (°)	0° (horizontal)	90° (vertical)
Mixture liquid velocity V_m (m/s)	0.2-2.0	0.5-1.5
Water cut (%)	0.5-20	1-20
Number of test points	76	41

behavior were tested. The iron counts, associated with each flow/wetting condition were measured over a sufficiently long period of time (typically 10 h) and correlated with the corrosion rate.

Test Matrix

In this work, oil-dominated flow in horizontal and vertical pipe was experimented with water cut ranging from 0.5% to 20%. Two types of measurements namely flow pattern and surface wetting were taken as per the experimental design matrix listed in Table 2. For each series of experiments, the test sequence was performed by incrementing the water cut at a given fixed mixture liquid velocity V_m, which is the sum of superficial oil and water velocities ($V_m = V_{so} + V_{sw}$). The flow pattern was recorded by the high-speed camera through the PVC transparent pipe, while the wetting data were measured by the conductivity pins once the flow was fully developed and in steady state. All flow and wetting experiments were repeated twice or more throughout the work. Flow patterns and wetting were carefully analyzed from thousands of close-up frames and wetting snapshots, combined with visual observation and experimental notes.

In Table 3, four cases (a) through (d) of horizontal oil-water flow conditions were experimented in the corrosion measurements, along with the observed flow patterns and surface wetting. The flow conditions were chosen in order to study the influence of different flow patterns and surface wetting on the rate of iron dissolution in CO_2 environment. At each condition, water was sampled from the oil-water separator at every 2-h interval, up to a total of 10 h. The total iron counts in the sampled solution were measured using ferrozine in a spectrophotometer apparatus.

TABLE 3
Test Matrix of Iron Counts for Four Different Flow Conditions

Mixture Liquid Velocity V_m (m/s)	Water Cut (%)	Observed Flow Pattern
(a) 0.5	10	Stratified with mixing layer
(b) 1.0	10	Stratified with mixing layer
(c) 1.0	1	Semi-dispersed
(d) 1.5	1	Dispersed

RESULTS AND DISCUSSION

Horizontal Flow Patterns

High-speed camera images of horizontal flow patterns are presented in Figure 6. The flow pattern results were grouped from low to high mixture liquid velocities V_m. For each series of results, the flow patterns are shown in the order of increasing water cuts. Keeping $V_m \leq 0.7$ m/s, various forms of separated flow patterns were observed for all tested water cuts as the flow is gravity dominated at low liquid velocities.[2] *Stratified smooth* (*ST-S*) flow patterns were seen at the lowest V_m of 0.2 m/s, where the oil/water interface was in a form of smooth interfacial waves as a result of low turbulence in the gravity-dominated flow. *Stratified-globules* (*ST-G*) flow patterns were seen at slightly higher V_m of 0.5 m/s to 0.7 m/s at low water cut, where the turbulence in the flow broke up the water phase into swarms of globules or droplets. The turbulent forces tended to disperse the water but were insufficient to counteract the settling tendency of gravity forces. Larger water globules were observed to flow alongside with swarms of densely packed small droplets in the lower pipe section, while oil phase remained continuous, flowing on top. As the water cut further increased, some elongated globules coalesced into semi-continuous streams of water snaking unstably at the pipe bottom. Increasing the water cut above 10%, *stratified with mixing layer* (*ST-M*) flow patterns were observed in which a continuous water layer flowed at the pipe bottom, continuous oil phase flowed on top, and a dispersion layer at the intermediate oil/water interface. The dispersion layer was similar to an emulsion layer consisting of both water-in-oil droplets and oil-in-water droplets, with the water droplets larger than the oil droplets. The generation of droplets at the interface boundary was thought to be the result of mutual shearing of both continuous phases, leading to dispersion of droplets by the interfacial turbulence.[2] The constant dynamic disturbances occurring within the interface reduced the likelihood of droplets to coalesce with the continuous phase. Increasing the mixture liquid velocity seemed to increase the mixing layer thickness.

At $V_m = 1$ m/s with 1% water cut, the low amount of water lost its continuity as the dominant oil flow became sufficiently intense to disperse the water as droplets. Gravitational pull caused an inhomogeneous spatial distribution of the droplets, resulting in a *semi-dispersed* (*S/D*) flow pattern in which water was sparsely dispersed in the upper pipe section, but more populated in the lower pipe section. By increasing water cut to 5%, swarms of water globules and droplets were observed to agglomerate at the pipe bottom. Beyond 10% water cut, a continuous water layer could be seen, along with a relatively thick dispersion layer at the interface, characterized as *stratified with mixing layer* (*ST-M*). By raising V_m to 1.5 m/s and above, a

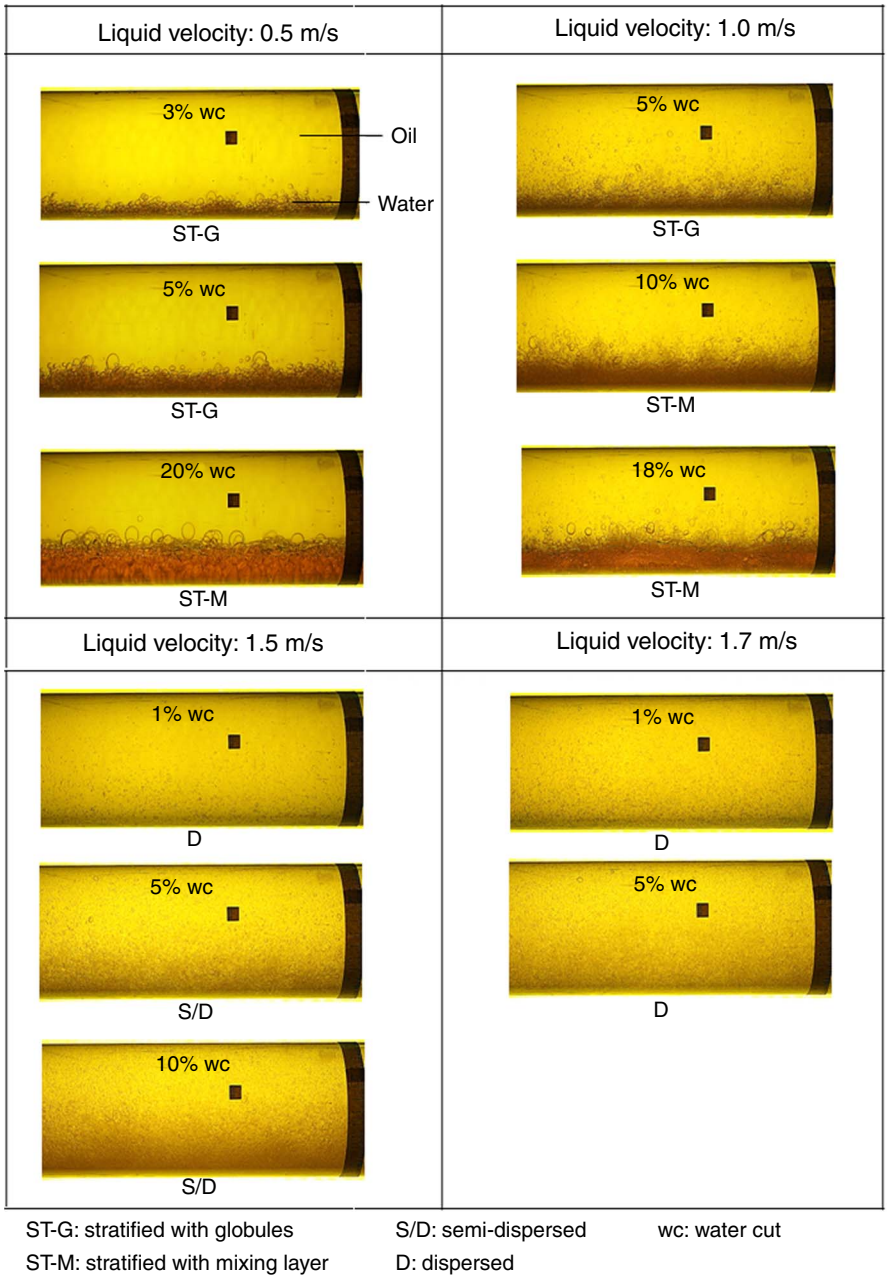

FIGURE 6. *Images of horizontal oil-water flow patterns taken by high-speed camera for liquid velocities V_m from 0.5 m/s to 1.7 m/s and water cuts from 5% to 20%.*

full dispersed flow pattern could be observed, where the water phase was dispersed and suspended evenly across the pipe section by the intense flow. With a slight rise of water cut above 1%, the flow pattern gradually transitioned to semi-dispersed flow in which water droplets were increasingly populated in the lower pipe section as a result of gravitational pull. Both dynamic pressure and body forces acted simultaneously on the droplets. The former tended to convect the droplets, while the latter dictated the settling of droplets by gravity. Each droplet exerted surface tension force to counteract the external forces and maintain its sphericity. Some of the partially lifted water droplets were seen to deviate from the flow path and momentarily "touch" the pipe wall. The flow pattern results are plotted in a flow pattern map shown in Figure 7. An empirical transition line (dashed line), delineating the stratified and dispersed flows, is included in the flow pattern map.

Surface Wetting in Horizontal Flow

By analyzing the surface wetting behavior obtained from the conductivity pins at various flow

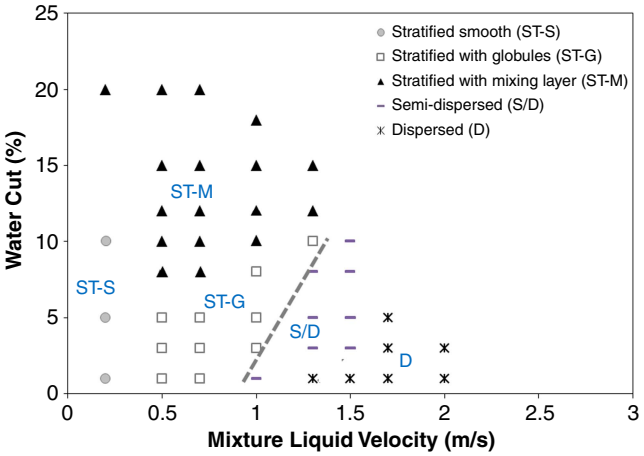

FIGURE 7. *Flow pattern map for horizontal oil-water flow in 0.1 m ID pipe.*

conditions, four categories of surface wetting regimes can be identified and depicted in Figure 8:

- *Stable water wet*: some pins are water wet and stay water wet.
- *Unstable water wet*: more than 3% of the pins stay water wet, some pins change intermittently between oil wet and water wet.
- *Unstable oil wet*: not more than 3% of the pins stay water wet, some pins change intermittently between oil wet and water wet.
- *Stable oil wet*: all pins are oil wet.

The response from the conductivity pins, representative of the surface wetting, varies in space and time. The signals from each wetting case were typically measured for 5 min at 1 s intervals and the wetting snapshots were then carefully analyzed to ascertain the wetting regime according to the above criteria. It is worth noting that both *unstable oil wetting* and *unstable water wetting* display intermittent behavior but with different degree of wetting intermittency. In previous work, these two wetting behaviors were collectively termed as intermittent wetting.[1] However, it is recognized that a case where most pins are oil wet with few pins showing intermittent wetting is quite different from another case where most pins are water wet with few pins showing intermittent wetting. From the corrosion standpoint, the latter case would have a higher likelihood of corrosion because the probability of free water wetting the steel surface for extended periods of time is higher, hence enhancing the replenishment of corrodents at the surface. The pin system was also built with redundancy by mounting a large number of conductivity pins onto the interior pipe wall. In this work, it was established from the experiment that over 3% of the positive pin response is taken as water wetting behavior to eliminate the possibility non-responsive pins or outliers.[16]

Using the proposed scheme of wetting regimes, the wetting behavior in horizontal flow can be plotted in a surface wetting map as shown in Figure 9, where each data point indicates one of the four possible wetting regimes at a given flow condition. The wetting results can be cross-correlated with the flow pattern map in Figure 7. In general, the surface wetting was affected by the hydrodynamics and flow patterns. For a separated flow pattern at low mixture liquid velocity V_m of 0.5 m/s, water wetting occurred at the 6 o'clock position in the horizontal flow. The area of water wetting location expanded as the water cut increased. By slightly increasing the liquid velocity to $V_m = 0.7$ m/s, *unstable water wet* was seen at low water cut <5% and changed to *stable water wet* when the water cut increased. The *unstable water wet* behavior at low water cut can be linked to the presence of swarms of closely dispersed water droplets intermittently "touching" along the pipe bottom. When transitioning to semi-dispersed and dispersed flow patterns at higher mixture liquid velocity V_m of 1.5 m/s, the wetting showed gradual transition from unstable water wet to unstable oil wet behavior. *Stable oil wet* was only observed at the lowest 0.5% water cut, which meant water was completely entrained and kept off of the pipe wall. However a slight rise of water cut to 1% resulted in *unstable oil wet* in this range of velocities. The *unstable oil wet* behavior was more prevalent at higher mixture liquid velocity with low water cut, while *unstable water wet* behavior was dominant at higher water cut >5% when the intermittency of water wetted pins became more frequent as the dispersed flow pattern transitioned to semi-dispersed flow pattern. As evident from the flow visualization, the unstable wetting behavior can be explained by the possibility of water droplets settling down and momentarily "touching" the wall before they were lifted away. The findings revealed that the local water distribution on the wall was intermittent and unstable in nature at such flow conditions.

An experimental wetting transition line between *unstable oil wet* and *unstable water wet* is included in the wetting map shown in Figure 9. In view of the contrasting wetting intensities between these two wetting behaviors, the delineation is performed to distinguish the former as "oil wetting" condition where the corrosion is unlikely to occur and the latter as "water wetting" condition where the corrosion is likely to occur.

Figure 10 shows the previous wetting results using the old conductivity pin section under similar light refined paraffinic oil water system.[1] As shown in Figure 10, the previous wetting results displayed much prominent oil wetting behavior at lower water cuts (<3%) and high mixture liquid velocity (>1.7 m/s), while the present results showed much pronounced intermittent wetting varying between *unstable oil wet* and *unstable water wet* behaviors. This could be attributed to the increased sensitivity of the new conductivity pin system that could detect traces of water on the

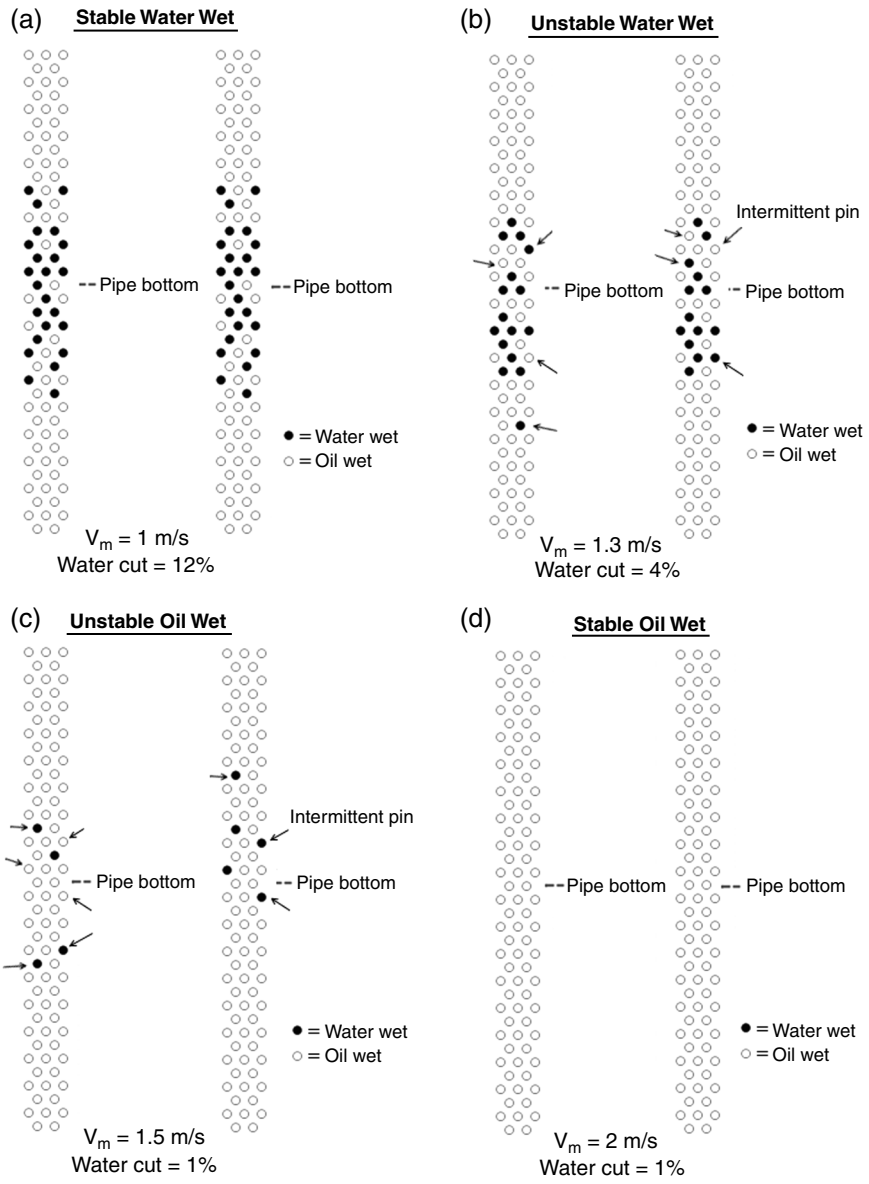

FIGURE 8. *Four categories of surface wetting: (a) stable water wet, (b) unstable water wet, (c) unstable oil wet, and (d) stable oil wet. Arrows (→) indicate intermittent pins switching between oil wet and water wet.*

wall and improved surface preparation of the test section at the start of experiments by polishing followed by 30 min rinsing with slugs of oils.

Vertical Flow Pattern

This section presents the vertical oil-water flow pattern images from the high-speed camera, depicting two subgroups of oil-dominated vertical flow patterns. At liquid velocity V_m of 0.5 m/s from 3% to 20% water cut in Figure 11, *dispersed globules* flow pattern was observed. At a low water cut of 3%, the water was dispersed in the form of globules/droplets sparsely distributed within the continuous bulk oil flow. The droplets/globules were rounded and relatively small. At 5% water cut, clusters of large water globules can be seen to flow along with the dispersed droplets. The water globules were in flat ovals similar to a "hamburger" shape. They flowed in an upward path with very little sideways swerving. As the water cut increased to 10%, the water globules grew into a larger irregular shape that deformed unsteadily as they flowed upward. The water globules were observed to move much slower than the droplets, showing noticeable slippage. Forces countering the individual droplet motion were the viscous drag and gravity forces. At the highest tested water cut of 20%, the water globules appeared to cease to grow in size. The droplets became rounded: more closely packed and became harder to observe as discrete droplets. The in situ

volume fraction of the dispersed phase exceeded the input water cut, resulting in a densely packed dispersion. It was believed that the densely packed droplets bounded by the finite pipe diameter restricted the droplet mobility and growth. These droplets, being closely packed, were likely to "touch" and wet the pipe when they were flowing in close proximity to the bounded wall. No water slug/churn was observed at any tested water cuts.

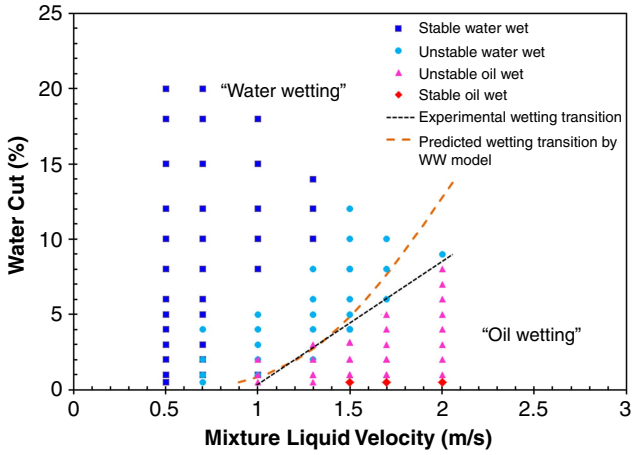

FIGURE 9. *Surface wetting map for horizontal light refined paraffinic oil water flow using new pins design.*

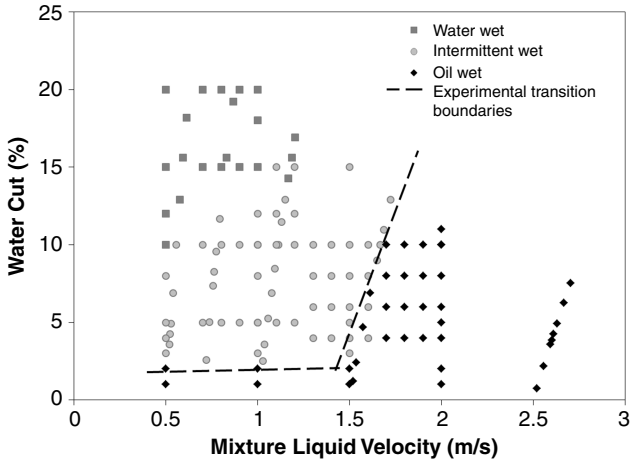

FIGURE 10. *Surface wetting map of horizontal light refined paraffinic oil water flow using previous pins design.*[1]

The flow pattern data at V_m of 1 m/s are displayed in Figure 12, showing a gradual flow pattern transition from *dispersed globules* to *dispersed droplets*, as evidenced by the absence of large globules. Because of higher liquid velocity, the increased turbulence resulted in a dispersion of fine water droplets that distributed uniformly across the pipe, characterized as *dispersed droplets* flow pattern. At 1% to 3% water cuts, the water droplets were sparsely distributed across the pipe. Small water droplets and some irregularly shaped globules flowed upward. As water cut increased to 10%, the dispersed water droplets became slightly larger and denser. The dispersed droplets were seen to flow upward with very little slippage with respect to the bulk oil flow. At high water cut of 18%, the droplets were similar in size to that observed for 10% water cut but became more closely packed. Within the duration of droplets passing through the view box, they did not seem to coalesce into a larger droplet.

All of the vertical oil-water flow pattern data are plotted in a flow pattern map in Figure 13, showing the flow patterns of *dispersed globules* at a lower range of V_m and *dispersed droplets* at a higher range of V_m. At $V_m = 1.5$ m/s, the visibility was compromised by the unwanted entrainment of air into the bulk flow sucked from the air cap in the oil tank. This affected the apparent density/viscosity of the phases.

Surface Wetting in Vertical Flow

The vertical flow wetting data obtained from the 360° pins section were analyzed and plotted on a surface wetting map in Figure 14. Each data point in the wetting map represents one of the four possible wetting regimes as defined in the previous section. Results showed that *stable oil wet* generally prevailed for vertical oil-water flow, which means water is kept from

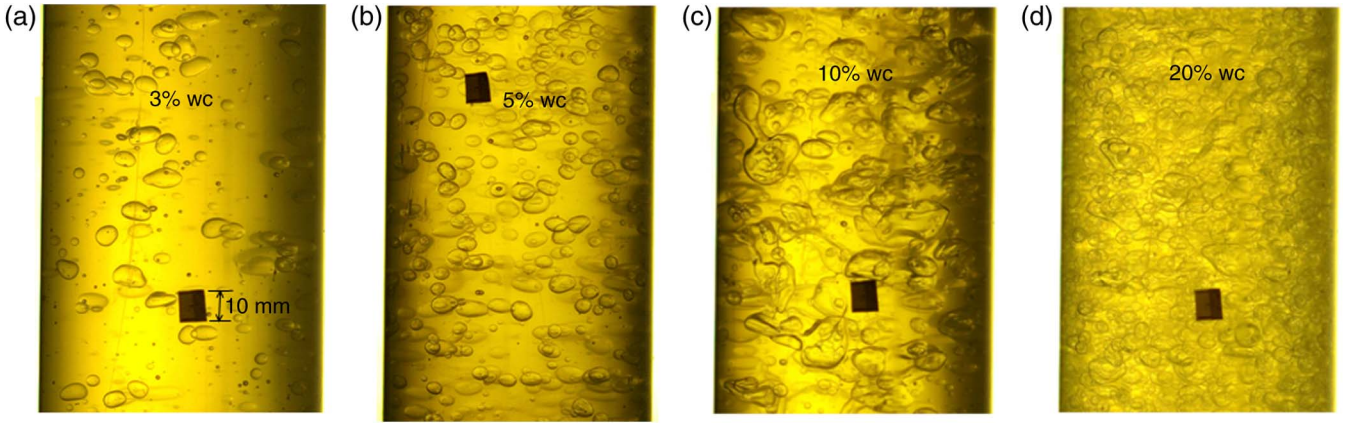

FIGURE 11. *Images of vertical oil-water flow patterns for $V_m = 0.5$ m/s from 3% to 20% water cuts.*

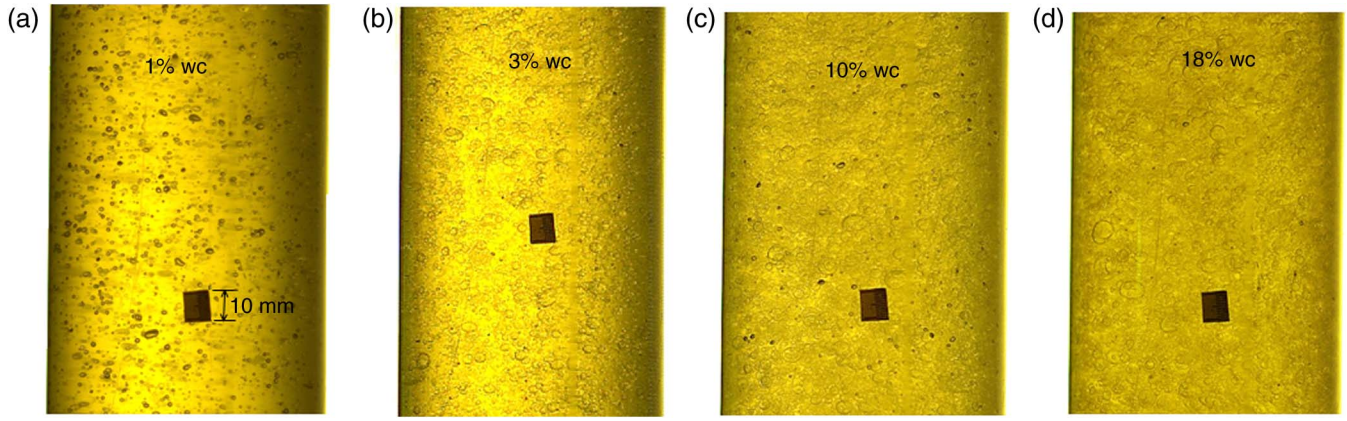

FIGURE 12. *Images of vertical oil-water flow patterns for V_m = 1 m/s from 1% to 18% water cuts.*

wetting the pipe wall by the continuous oil phase. The surface wetting changed to *unstable oil wet* when the water cut increased beyond 14% at liquid velocities V_m of 0.5 m/s to 1 m/s. At those flow conditions, the wetting results indicated that most of the pipe wall area was oil wet with few locales (indicated by pins) changing intermittently and randomly. The occurrences of water wetted locales were limited, suggesting the *unstable oil wet* condition was as good as the *oil wet* condition. With an increase in liquid velocity, the droplet size was reduced as a result of the higher turbulent breaking force that acted against the droplet surface tension. However, the velocity did not seem to have a remarkable influence on the surface wetting. The water phase was mostly kept from the pipe wall regardless of the input velocity, indicating the flowing water droplets seldom deviated from the streamline of a straight flow path. Upon examining the high-speed camera recordings, the oil wetting behavior at low water cut can be explained by the sparse distribution of water droplets/globules that moves in a relatively straight upward path, with little likelihood of impinging sideways onto the wall as the gravity is not acting to pull the water to the wall and the viscous drag tends to guide the fluid particle along the streamlines of bulk flow. Increasing the water cut beyond 14% caused the dispersed droplets to coalesce to a larger size and pack more closely to each other. These crowded globules near the wall were likely to contact and wet the pipe wall when they were flowing in close proximity to the wall, resulting in *unstable oil wet*. However, the wetting was minimal as the Saffman lift force and lubrication force may exist to prevent the droplets from approaching too close to the solid wall.[17] In addition, the *unstable oil wet* behavior appeared to be slightly more prevalent at lower liquid velocity compared to higher liquid velocity. For globules with irregular shapes, they were relatively large and moved slowly; one needs to consider the effect of gravity and momentum, as they are likely to deviate from the

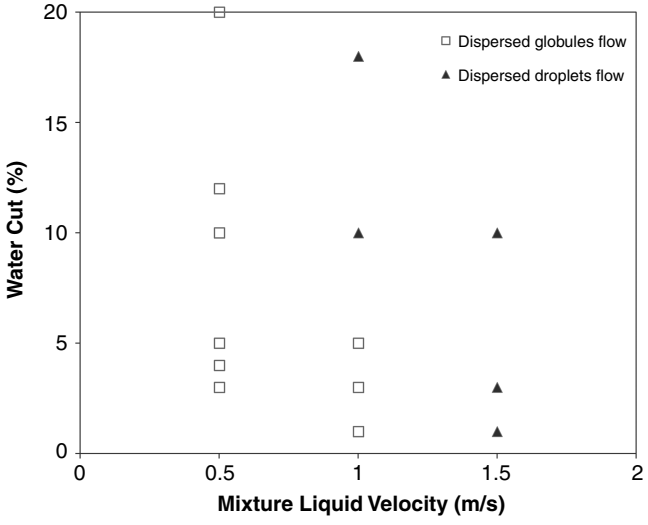

FIGURE 13. *Flow pattern map for vertical light refined paraffinic oil water flow in 0.1 m ID pipe.*

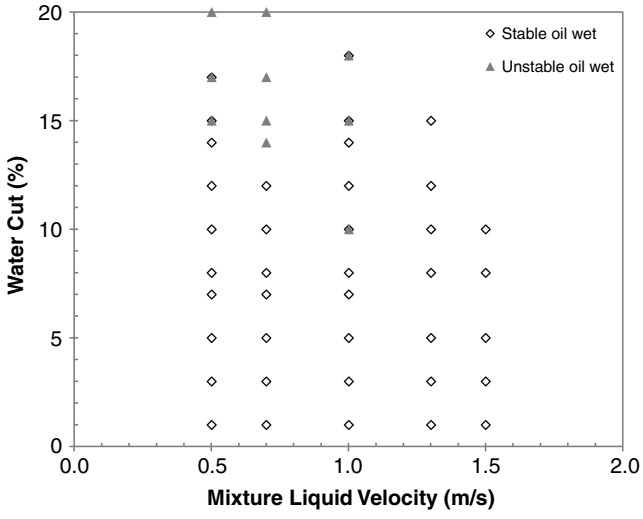

FIGURE 14. *Surface wetting map for vertical light refined paraffinic oil water flow in 0.1 m ID pipe.*

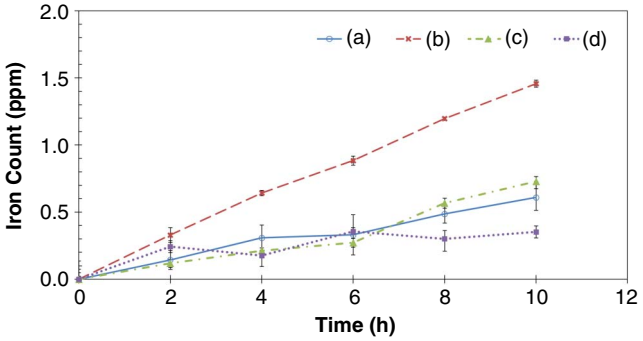

FIGURE 15. *Variations of iron counts over time for the four different flow conditions. For details see Table 4.*

flow streamlines. On the other hand, the smaller droplets entrained in fast flowing oil stream may be thought to have less likelihood of collision to the wall resulting from their smaller inertia and more rounded geometry to travel in a straight path.

Two remarks must be made regarding the vertical oil-water low. First, the prevailing oil wetting was observed to persist for a test section that was freshly polished. Once water has wetted the steel wall, which is naturally more hydrophilic, the water wetting prevailed and was not easily displaced by the continuous oil flow alone. Second, truly vertical pipe rarely exists in the production fields. It had been experimentally tested that if the test loop were slightly inclined off-axis from the vertical plane, the risk of water wetting the wall was increased because of the effect of gravity pulling down the water to wet the inclined wall.

Iron Counts

The iron count measurements taken throughout the 10 h flow loop experiments for four flow cases, denoted as (a) through (d), were plotted in Figure 15. The summarized results are tabulated in Table 4. The iron count measurements appeared to depend on the flow velocity and water distribution. Inspection of the results shows that flow Case (b) with V_m = 1 m/s and 10% water cut resulted in the highest rise in iron counts, followed by the three other cases, which overlapped with each other. Generally, one can correlate a more rapid increase in iron counts with an increased rate of corrosion. However, in the case of multiphase flow, the area of the steel surface wetted by water also plays a role as it changes the corroding surface area.[1,16] The most rapid increase in iron counts seen for Case (b) which has the combination of high velocity (1 m/s) and high water cut (10%). The observed flow was stratified with mixing layer and the wetting was stable water wetting. The other cases, with either lower velocity or lower water cut, resulted in a lower iron count rise. One can speculate that Case (a), which has a high water cut (10%), resulted in lower corrosion rate because of lower velocity (0.5 m/s), and consequently lower mass transfer rate. On the other hand, Cases (c) and (d) conducted at higher velocities (1 m/s and 1.5 m/s, respectively) both had low water cuts (1%), which caused a much smaller water-wetted area of the pipe wall, resulting in a lower corroding area and lower iron counts. For the dispersed flow pattern in Case (d), the iron counts showed a near flatline trend. The results implied that corrosion rate was negligible if the water was entrained and kept away from the pipe wall.

It is noted that iron counts are an indirect way to correlate surface wetting with corrosion rate. For a flow loop setting with large volume of circulating fluids such as the one used in the present study, the iron count results can have a considerable margin of uncertainty. It was not possible to attribute the rise in iron counts solely to the surface wetting effect, as other factors may interfere.[16] Therefore, the iron count results were used to complement the findings obtained from other techniques, described earlier.

Modeling

Cai, et al., formulated mechanistic water wetting (WW) model based on the liquid-liquid flow pattern transition work by Brauner to predict the critical entrainment velocity required to disperse the water phase.[1,18] The premise of the model was that the turbulent fluctuation energy from the oil phase was solely expended to counteract the surface energy and break up the water into discrete droplets. If all of the free water is entrained by the oil, then water will be kept off from the wall, leading to oil wetting behavior, and vice versa for water wetting if free water drops out from the oil and comes in contact with the wall. Following this model, the criterion for transition is determined by evaluating the maximum droplet size d_{max} and critical droplet size d_{crit}. The model was based on the mechanistic formulations originating from the droplet breakup mechanism proposed by Hinze and later modified by Brauner to account for dense droplet

TABLE 4

Experimental Details and Measured Iron Counts at the 10th Hour for Four Different Flow Conditions

V_m (m/s)	Water Cut (%)	Iron Counts (ppm)	Flow Pattern	Surface Wetting
(a) 0.5	10	0.61	Stratified with mixing layer	Stable water wet
(b) 1.0	10	1.46	Stratified with mixing layer	Stable water wet
(c) 1.0	1	0.73	Semi-dispersed	Unstable water wet
(d) 1.5	1	0.35	Dispersed	Unstable oil wet

dispersion.[18-19] The maximum droplet size d_{max} is calculated using the following expressions in Equations (1) and (2):

$$d_{max} = 2.93\, C_H^{-0.6} \left(\frac{\rho_c}{\sigma}\right)^{-0.6} \left(\frac{1-\varepsilon_d}{\varepsilon_d}\right)^{-0.6} \bar{e}^{-0.4} \quad (1)$$

where ρ_c is the density of the continuous phase, σ is the interfacial tension, ε_d is the input water cut, C_H is the empirical constant taken as 1, and $\bar{e}$ is the mean energy dissipation rate related to the frictional pressure gradient as follows:

$$\bar{e} = \left(\frac{dP}{dL}\right) \frac{U_c}{\rho_c \varepsilon_c} \quad (2)$$

The droplets resulting from the breakup in the turbulent pipe flow can distribute differently depending on the force balance between the turbulent fluctuations and the forces resulting from gravity or deformation effect, represented by calculating the critical droplet size, d_{crit}, as follows, which is the minimum of two values as suggested by Barnea, et al.:[20]

$$d_{crit} = \text{Min}\left(d_{cg} = \frac{3}{8}\frac{\rho_O U_{SO}^2 f}{|\rho_W - \rho_O| g \cos\theta}, \; d_{c\sigma} = \sqrt{\frac{4\sigma}{|\rho_W - \rho_O| g \cos\theta'}}\right) \quad (3)$$

where ρ_w is the water density, d_{cg} is the critical size resulting from gravity/buoyancy forces which act predominantly in horizontal oil-water flow, and $d_{c\sigma}$ is the critical size resulting from deformation of a spherical droplet which is important in vertical or near-vertical flow.

The wetting transition criterion is assumed to coincide with the wetting transition. The transition from water wetting to oil wetting takes place when the turbulence of the oil phase is intense enough to break up the water phase into droplets not larger than d_{max} and smaller than d_{crit}. Hence, the critical entrainment velocity required to entrain the water phase can be calculated by solving the following criterion:[21]

$$d_{max} \le d_{crit} \quad (4)$$

On the other hand, water drops out from the oil and wets the wall if $d_{max} > d_{crit}$. The complete WW model description is given by Cai, et al.[21] By using the WW model, a predicted wetting transition line can be generated based on the input horizontal oil-water flow conditions and plotted on the surface wetting map, as shown in Figure 9. The predicted transition line can be viewed as the critical entrainment velocity required to disperse the discontinuous phase at given water cut. Comparing it with the empirical wetting transition line, the model shows reasonable agreement in the delineation between unstable water wet and unstable oil wet. It predicts well for cases at low water cut until 5% when it becomes somewhat less conservative at a higher range of water cuts.

CONCLUSIONS

❖ For the oil-water flow experiments, five types of flow patterns were reported in horizontal flow. They are *stratified smooth*, *stratified with globules*, *stratified with mixing layer*, *semi-dispersed*, and *dispersed* flow patterns. Two types of flow patterns, *dispersed globules* and *dispersed droplets*, were reported in vertical flow.

❖ In horizontal oil-water flow, the pipe bottom was predominantly wetted by the free water layer when the flow was gravity dominated and the phases were separated at low mixture liquid velocity $V_m \le 0.7$ m/s.

❖ For semi-dispersed and dispersed flow patterns observed at higher V_m of 1 m/s and above, the water was generally entrained by the turbulent oil stream. *Unstable oil wet* was observed at low water cut and became *unstable water wet* as water cut increased. Nonetheless, the wetting showed gradual transition from water wet to unstable oil wet as the mixture liquid velocity was increased. The unstable wetting behavior can be attributed to the presence of a swarm of water droplets settling down and momentarily touching the pipe. Not all water was fully entrained in dispersed flow, as traces of water can still be found to wet the surface intermittently, causing unstable wetting.

❖ The intermittency and unstable nature of the intermittent wetting can be categorized as *unstable water wet* and *unstable oil wet*. From the corrosion perspective, the former postulates corrosion is likely to take place, while the latter is unlikely for corrosion to occur.

❖ In vertical flow, the dispersed water droplets/globules tend to travel in a straight line without much swerving. The wetting was predominantly oil wet across the tested velocity range. The change of liquid velocity did not seem to affect the wetting behavior. At low V_m with water cut >15%, unstable water wetting was observed. This can be explained by the occurrence of densely distributed water droplets/globules close to the pipe wall.

❖ The iron count results appeared to depend on the flow velocity and water distribution. The corrosion rate was highest when the oil-water flow had the combination of high velocity (1 m/s) and high water cut (10%), corresponding to water wetting condition.

❖ A mechanistic model for predicting the wetting transition was applied to compare the predicted critical entrainment velocity with the empirical data, which showed reasonable agreement.

ACKNOWLEDGMENTS

The work presented in this paper was part of a joint industry project named the Water Wetting project undertaken at the Institute for Corrosion and Multiphase Technology at Ohio University. The authors wish to

thank the financial support and technical directions from the sponsoring companies: BP, ConocoPhilips, ExxonMobil, Petrobras, Saudi Aramco, and TOTAL. Support from Universiti Teknologi Petronas is much appreciated.

REFERENCES

1. J. Cai, C. Li, X. Tang, F. Ayello, S. Richter, S. Nesic, *Chem. Eng. Sci.* 73 (2012): p. 334-344.
2. J. Trallero, C. Sarica, J. Brill, *SPE Prod. & Fac.* 12, 3 (1997): p. 165-172.
3. J. Flores, X. Chen, C. Sarica, J. Brill, *SPE Prod. & Fac.* 14, 2 (1999): p. 102-109.
4. G.W. Govier, G.A. Sullivan, R.K. Wood, *Can. J. Chem. Eng.* 39, 2 (1961): p. 67-75.
5. H. Shi, J. Cai, W.P. Jepson, *J. Energy Resources Technol.* 123, 4 (2001): p. 270-276.
6. M. Vielma, S. Atmaca, C. Sarica, H.-Q. Zhang, *SPE Projects, Fac. & Construction* 3, 4 (2008): p. 3133-3143.
7. A. Cartellier, J.L. Achard, *Rev. of Scientific Instruments* 62, 2 (1991): p. 279-303.
8. J. Trallero, "Oil-Water Flow Patterns in Horizontal Pipes" (Ph.D. diss., The University of Tulsa, 1995).
9. A. Valle, "CO2-Corrosion and Water Distribution in Two Phase Flow of Hydrocarbon Liquids and Water," CORROSION 2000, paper no. 047 (Houston, TX: NACE International, 2000).
10. P. Angeli, G.F. Hewitt, *Int. J. Multiphase Flow* 26 (2000): p. 1117-1140.
11. J. Cai, S. Nesic, C. Li, X. Tang, F. Ayello, C. Ivan, T. Cruz, J. Al-Khamis, "Experimental Studies of Water Wetting in Large-Diameter Horizontal Oil/Water Pipe Flows," SPE Annual Technical Conference and Exhibition (ATCE), 2005, p. 719-731.
12. C. Li, X. Tang, F. Ayello, J. Cai, S. Nesic, C.I. Cruz, J. Al-Khamis, "Experimental Study on Water Wetting and CO2 Corrosion in Oil-Water Two-Phase Flow," CORROSION 2006, paper no. 595 (Houston, TX: NACE, 2006).
13. F. Ayello, C. Li, X. Tang, J. Cai, S. Neic, C.I. Cruz, J. Al-Khamis, "Determination of Phase Wetting in Oil-Water Pipe Flows," CORROSION 2008, paper no. 566 (Houston, TX: NACE, 2008).
14. X. Tang, C. Li, F. Ayello, J. Cai, S. Nesic, "Effect of Oil Type on Phase Wetting Transition and Corrosion in Oil-Water Flow," CORROSION 2007, paper no. 170 (Houston, TX: NACE, 2007).
15. K. Kee, R. Sonja, M. Babic, S. Nesic, "Flow Patterns and Water Wetting in Oil-Water Two Phase Flow–A Flow Loop Study," CORROSION 2014, paper no. 4068 (Houston, TX: NACE, 2014).
16. K.E. Kee, "A Study of Flow Patterns and Surface Wetting in Gas-Oil-Water Flow" (Ph.D. diss., Ohio University, 2014).
17. M.A. Hubbe, H. Chen, J.A. Heitmann, *Bio Resources* 4, 1 (2009): p. 405-451.
18. N. Brauner, *Int. J. Multiphase Flow* 27, 5 (1986): p. 885-910.
19. J.O. Hinze, *AICHE J.* (1955): p. 289-295.
20. D. Barnea, O. Shoham, Y. Taitel, *Int. J. Multiphase Flow* 12, 5 (1986): pp. 733-744.
21. J. Cai, S. Nesic, C. de Waard, "Modeling of Water Wetting in Oil-Water Pipe," CORROSION 2004, paper no. 663 (Houston, TX: NACE, 2004).